Molecular Cell
Article

Caspase-2-Mediated Cleavage of Mdm2 Creates a p53-Induced Positive Feedback Loop

Trudy G. Oliver,[1,4] Etienne Meylan,[1,5] Gregory P. Chang,[1] Wen Xue,[1] James R. Burke,[1] Timothy J. Humpton,[1] Diana Hubbard,[2] Arjun Bhutkar,[1] and Tyler Jacks[1,3,*]
[1]Koch Institute for Integrative Cancer Research, Massachusetts Institute of Technology, Cambridge, MA 02139, USA
[2]Eli and Lily Broad Institute of Harvard and Massachusetts Institute of Technology, Cambridge, MA 02139, USA
[3]Howard Hughes Medical Institute, Chevy Chase, MD 20185, USA
[4]Present address: Huntsman Cancer Institute and University of Utah, Salt Lake City, UT 84112, USA
[5]Present address: Swiss Institute for Experimental Cancer Research, Ecole Polytechnique Fédérale de Lausanne, Station 19, CH-1015 Lausanne, Switzerland
*Correspondence: tjacks@mit.edu
DOI 10.1016/j.molcel.2011.06.012

SUMMARY

Caspase-2 is an evolutionarily conserved caspase, yet its biological function and cleavage targets are poorly understood. Caspase-2 is activated by the p53 target gene product PIDD (also known as LRDD) in a complex called the Caspase-2-PIDDosome. We show that PIDD expression promotes growth arrest and chemotherapy resistance by a mechanism that depends on Caspase-2 and wild-type p53. PIDD-induced Caspase-2 directly cleaves the E3 ubiquitin ligase Mdm2 at Asp 367, leading to loss of the C-terminal RING domain responsible for p53 ubiquitination. As a consequence, N-terminally truncated Mdm2 binds p53 and promotes its stability. Upon DNA damage, p53 induction of the Caspase-2-PIDDosome creates a positive feedback loop that inhibits Mdm2 and reinforces p53 stability and activity, contributing to cell survival and drug resistance. These data establish Mdm2 as a cleavage target of Caspase-2 and provide insight into a mechanism of Mdm2 inhibition that impacts p53 dynamics upon genotoxic stress.

INTRODUCTION

The tumor suppressor function of p53 is dysregulated in the vast majority of human cancers via genomic loss, point mutation, or alterations in signaling components upstream of p53, such as ARF loss or Mdm2 amplification. As a transcription factor, p53 responds to cellular stress by inducing target genes that promote cell-cycle arrest, DNA repair, apoptosis, or senescence (Horn and Vousden, 2007; Menendez et al., 2009; Vousden, 2006). Because p53 plays a central role in determining cell-fate decisions, elucidation of the signaling circuitry that governs p53 function is critical for understanding tumorigenesis and manipulating p53 for therapeutic purposes.

Many factors regulate the stability and activity of p53, such as posttranslational modifications, protein-protein interactions, and subcellular localization (Manfredi, 2010; Marine and Lozano, 2010). The E3 ubiquitin ligase mouse/human double minute 2 (Mdm2/Hdm2) is a master regulator of p53 (Kruse and Gu, 2009; Marine and Lozano, 2010). Mdm2 controls p53 levels by targeting it for ubiquitin-mediated proteasomal degradation (Haupt et al., 1997; Kubbutat et al., 1997) and can bind p53 and inhibit its transcriptional activity (Momand et al., 1992). *Mdm2* is also a target gene of p53, establishing a negative feedback loop that inhibits p53 activity after DNA damage (Juven et al., 1993; Wu et al., 1993).

Both positive and negative feedback loops are prominent features of the autoregulation of the p53 pathway (Harris and Levine, 2005; Lu, 2010). Well-known examples are the negative feedback loops induced by the p53 target gene products Mdm2, Wip1, Pirh2, and Cop1 (Marine and Lozano, 2010). However, p53 target genes that function in positive feedback loops have also been identified. For example, the p53 target protein Wig-1 (ZMAT3) has been shown to increase p53 levels by enhancing *p53* messenger RNA (mRNA) stability (Vilborg et al., 2009), while 14-3-3 sigma inhibits Mdm2-mediated ubiquitination of p53 (Yang et al., 2003). Studies in single cells and mouse models have demonstrated that p53 activity is induced in oscillations or pulses, both in response to high levels of damage and during the cell cycle of normal unstressed cells (Batchelor et al., 2009; Hamstra et al., 2006; Loewer et al., 2010). Given the pulsatile dynamics of p53 signaling (Lahav et al., 2004), it may be essential that p53 induces its own negative and positive regulators that control, or are controlled by, the p53 response and ultimately define p53 activity.

The p53 target gene, *l*eucine-*r*ich repeats and *d*eath *d*omain containing (*Lrdd*), also known as *p*53-*i*nduced protein with a *d*eath *d*omain (*Pidd*), functions in apoptosis, NF-κB-mediated survival signaling, cell-cycle arrest, DNA repair, and drug resistance (Janssens et al., 2005; Lin et al., 2000; Logette et al., 2011; Oliver et al., 2010; Tinel and Tschopp, 2004). PIDD is a death domain protein that is autocatalytically cleaved into multiple fragments, generating PIDD-C and PIDD-CC (Tinel et al., 2007). PIDD-C is a component of the so-called PIDDosome complex with RIP1 and Nemo, which promotes cell survival via

NF-κB activation (Janssens et al., 2005). PIDD-CC activates the protease Caspase-2 in a cytoplasmic PIDDosome complex assembled by the adaptor protein, RAIDD/CRADD (Bouchier-Hayes et al., 2009; Park et al., 2007; Tinel and Tschopp, 2004). We recently discovered that *Pidd* is induced in murine chemoresistant tumors in vivo and can promote cell cycle arrest and drug resistance in human lung cancer cells (Oliver et al., 2010). The mechanism by which PIDD promotes cell-cycle arrest and drug resistance is unknown.

Caspase-2 is an evolutionarily conserved caspase with features of both initiator and executioner caspases, yet very few of its targets are known (Krumschnabel et al., 2009a, 2009b; Kumar, 2009; Vakifahmetoglu-Norberg and Zhivotovsky, 2010). For example, Caspase-2 cleaves Golgin-160, and this cleavage has been implicated in Golgi disintegration and the initiation of apoptosis (Mancini et al., 2000). Caspase-2-mediated cleavage of Bid has been shown to promote cytochrome *c* release at the mitochondria during apoptosis (Guo et al., 2002; Upton et al., 2008). Additionally, Caspase-2 has been proposed to cleave RIP1 leading to NF-κB inhibition (Guha et al., 2010). Despite early evidence suggesting Caspase-2 plays a role in apoptosis, its function in this process remains controversial. *Caspase-2* null mice are viable, fertile, and display only mild defects in apoptosis (Bergeron et al., 1998). Caspase-2 can also influence cell-cycle regulation and DNA repair (Kumar, 2009). Recently, Caspase-2 has been implicated as a tumor suppressor gene as *caspase-2* null mouse embryonic fibroblasts (MEFs) exhibit increased proliferation and enhanced sensitivity to transformation (Ho et al., 2009). Tumor formation was accelerated in *caspase-2* null mice in an Eμ-myc model of lymphoma (Ho et al., 2009). Identification of new Caspase-2 cleavage targets should shed light on its biological functions.

Here, we demonstrate that DNA damage and PIDD-induced activation of Caspase-2 trigger cleavage of Mdm2, which reinforces p53 stability and activity in a positive feedback loop. This signaling pathway provides a mechanistic explanation for how transiently increased *PIDD* expression can protect cells from DNA damage.

RESULTS

PIDD Positively Regulates p53 Levels

The *PIDD* promoter contains a noncanonical p53 response element and is induced upon DNA damage and p53 activation (Jordan et al., 2008; Lin et al., 2000). We verified that *PIDD* is increased upon DNA damage by treating human non-small cell lung cancer (NSCLC) cell lines with a standard-of-care chemotherapy agent cisplatin. Consistent with published data, *PIDD* was highly induced in *p53* wild-type cells and much less so, or not at all, in *p53* null and mutant cells (Figure S1A available online). We next took advantage of a unique mouse model system that allows restoration of endogenous p53 to physiological levels (Ventura et al., 2007). Homozygous *p53*-Lox-Stop-Lox (LSL) mice ($p53^{LSL/LSL}$) crossed to $ROSA26^{CreERT2}$ mice are functionally *p53* null until addition of 4-hydroxytamoxifen (4-OHT), which activates Cre recombinase. Cre excises the Stop cassette and restores the *p53* locus to its wild-type state. Three independent mouse lung tumor cell lines driven by oncogenic $Kras^{G12D}$ ($Kras^{LA/+}$;$p53^{LSL/LSL}$;$ROSA26^{CreERT2}$ [KPR]) were treated with vehicle or 4-OHT and analyzed at multiple time points (Feldser et al., 2010). Restoration of *p53* led to *p21* induction and G1 cell-cycle arrest (Figures S1B and S1C). *Pidd* expression was significantly induced from 5- to 15-fold as early as 24 hr (Figure 1A). Thus, *Pidd* is induced both upon DNA damage as previously described and upon physiologically relevant *p53* restoration in cancer cells.

To examine the consequences of PIDD expression, we overexpressed Flag-tagged PIDD in human NSCLC cell lines that harbored *KRAS* mutations and were *p53* wild-type, null, or carrying point mutant alleles of *p53*. PIDD expression was confirmed in the nuclear and cytoplasmic fractions of nine independent cell lines (Figure S1D and data not shown). Exogenous PIDD expression led to a slower growth rate and G1 arrest in *p53* wild-type cells as we previously described (Oliver et al., 2010). Surprisingly, PIDD did not induce growth arrest in *p53* null or mutant cells (Figure 1B). We previously found that *p53* wild-type PIDD-expressing cells showed significantly increased cisplatin resistance compared to vector control cells (Oliver et al., 2010). In contrast, *p53* null or mutant PIDD-expressing cells did not exhibit increased cisplatin resistance, as indicated by a lack of change in the IC_{50} of PIDD-expressing versus control cells (Figure 1C). Thus, drug response in PIDD-expressing cells was significantly associated with *p53* status. Of nine cell lines, the one exception was the *p53* wild-type line, A427, in which PIDD overexpression did not induce cell cycle arrest or cisplatin resistance (see explanation in Figure S1D). Taken together, these data suggest that PIDD expression promotes cell-cycle arrest and drug resistance in a p53-dependent manner.

To test the requirement of p53 for PIDD-induced cell-cycle arrest, we compared cell growth rates in *p53* wild-type HCT116 colon cancer cells and isogenic *p53* null derivatives. Expression of PIDD significantly reduced cell growth rate in *p53* wild-type cells ($p < 0.02$) and had no effect in the absence of *p53* ($p > 0.38$) (Figure 1D), demonstrating that *p53* is required for PIDD-induced inhibition of the cell cycle.

To further investigate the relationship between PIDD and p53, we analyzed p53 protein levels in control and PIDD-expressing cells. In *p53* wild-type cells, PIDD expression led to increased nuclear p53 levels and an increase in nuclear p21, a canonical p53 target (Figure 1E). Levels of p53 and p21 protein did not change in *p53* null or mutant cells upon PIDD expression (Figure S1E). In *p53* wild-type cells, *p53* mRNA levels were unchanged upon PIDD expression, while *p21* mRNA was upregulated in a p53-dependent manner (Figure 1F), suggesting that PIDD leads to increased p53 protein stability and activity. Thus, PIDD, a target gene product of p53, can increase p53 protein levels in a positive feedback mode.

PIDD-Induced Growth Arrest and Cisplatin Resistance Depend on Caspase-2

The Caspase-2-PIDDosome is a high-molecular-weight complex composed of PIDD, the adaptor protein, RAIDD, and Caspase-2 (Tinel and Tschopp, 2004). This complex is assembled via death domain interactions between PIDD and RAIDD. RAIDD recruits Caspase-2 via their mutual caspase recruitment domains (CARDs) (Park et al., 2007). Formation of the

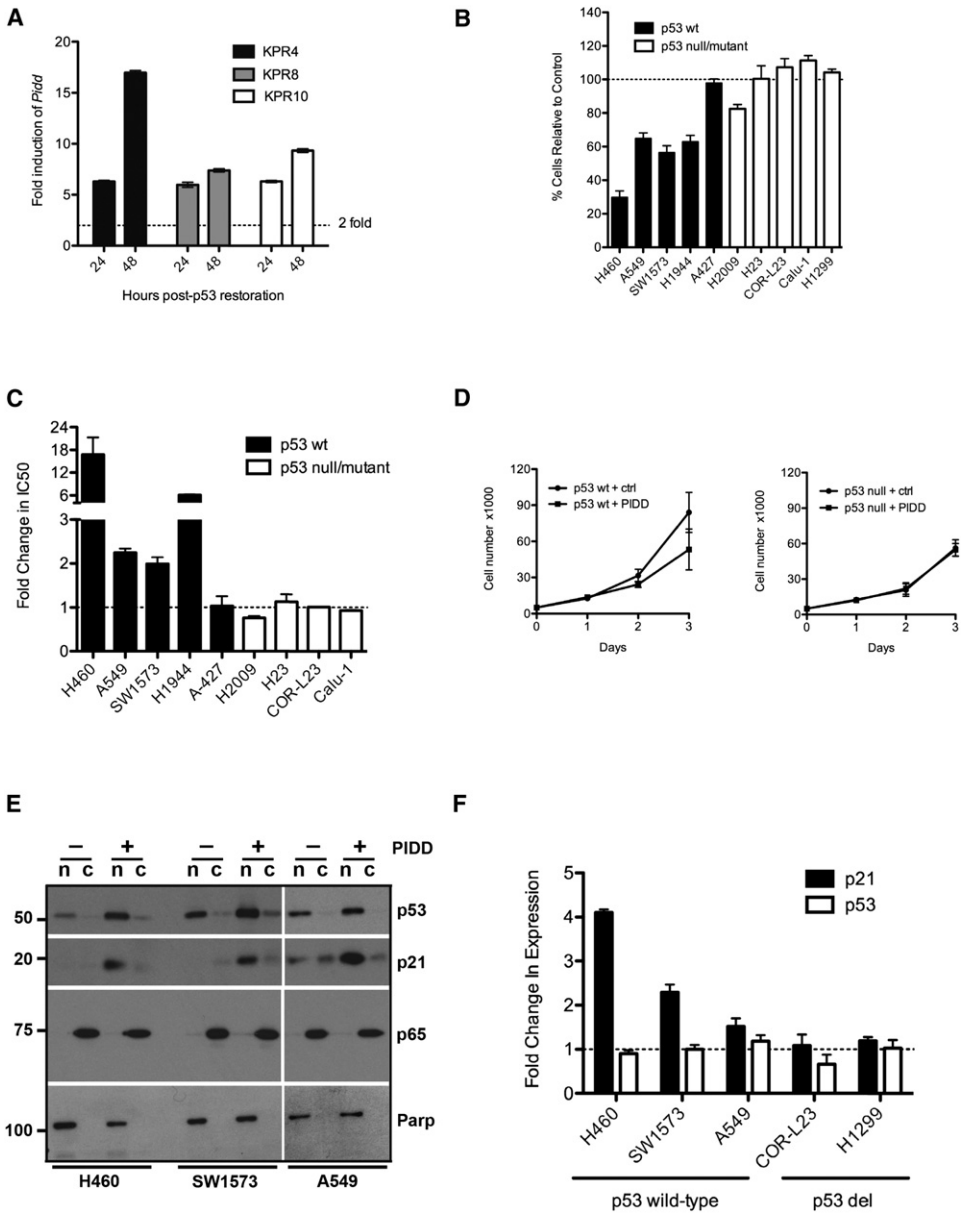

Figure 1. PIDD Positively Regulates p53 Levels

(A) *Pidd* levels analyzed by real time RT-PCR and normalized to *actin*; fold change of 4-OHT relative to vehicle control. n = 3.

(B) Cell number measured in triplicate of PIDD-expressing cells compared to control cells after 72 hr; n = 2, except for H1299, n = 1. Average percent cell number for PIDD-expressing cells compared to control for *p53* wild-type (66% ± 5%) versus *p53* null/mutant (100% ± 5%).

(C) IC_{50} for PIDD versus control cells after 48 hr cisplatin. Average data from two independent sets of cells performed in triplicate. Cisplatin-resistant *p53* wild-type lines (n = 4 of 5) versus *p53* null/mutant lines (n = 0 of 4) ($p < 0.01$, Chi Square and $p < 0.04$, Fisher's exact test).

(D) *p53* WT or null HCT116 cells expressing PIDD or vector. Cells counted in quadruplicate every 24 hr, n = 2. For *p53* WT cells, $p < 0.02$.

(E) Immunoblot of nuclear/cytoplasmic (n/c) fractions in control or PIDD-expressing cells. p65 and PARP serve as cytoplasmic and nuclear loading controls, respectively.

(F) Fold change in *p21* and *p53* mRNA levels in *p53* wild-type (H460, SW1573, A549) and *p53* mutant cells (COR-L23, H1299) in PIDD-expressing versus control cells. n = 3, normalized to *ACTIN*.

Error bars in all panels represent the mean ± standard deviation (SD). See also Figure S1.

PIDDosome activates Caspase-2 by proximity-induced dimerization and subsequent autoprocessing of pro-Caspase-2 (Bouchier-Hayes et al., 2009). We found that cytoplasmic pro-Caspase-2 was significantly reduced or absent in all cell lines upon ectopic PIDD expression, regardless of *p53* status (Figure 2A). Under different lysis conditions, the cleavage products of Caspase-2 that are generated during activation are detectable in total cell lysates as well (Figure S2). Transcriptional repression

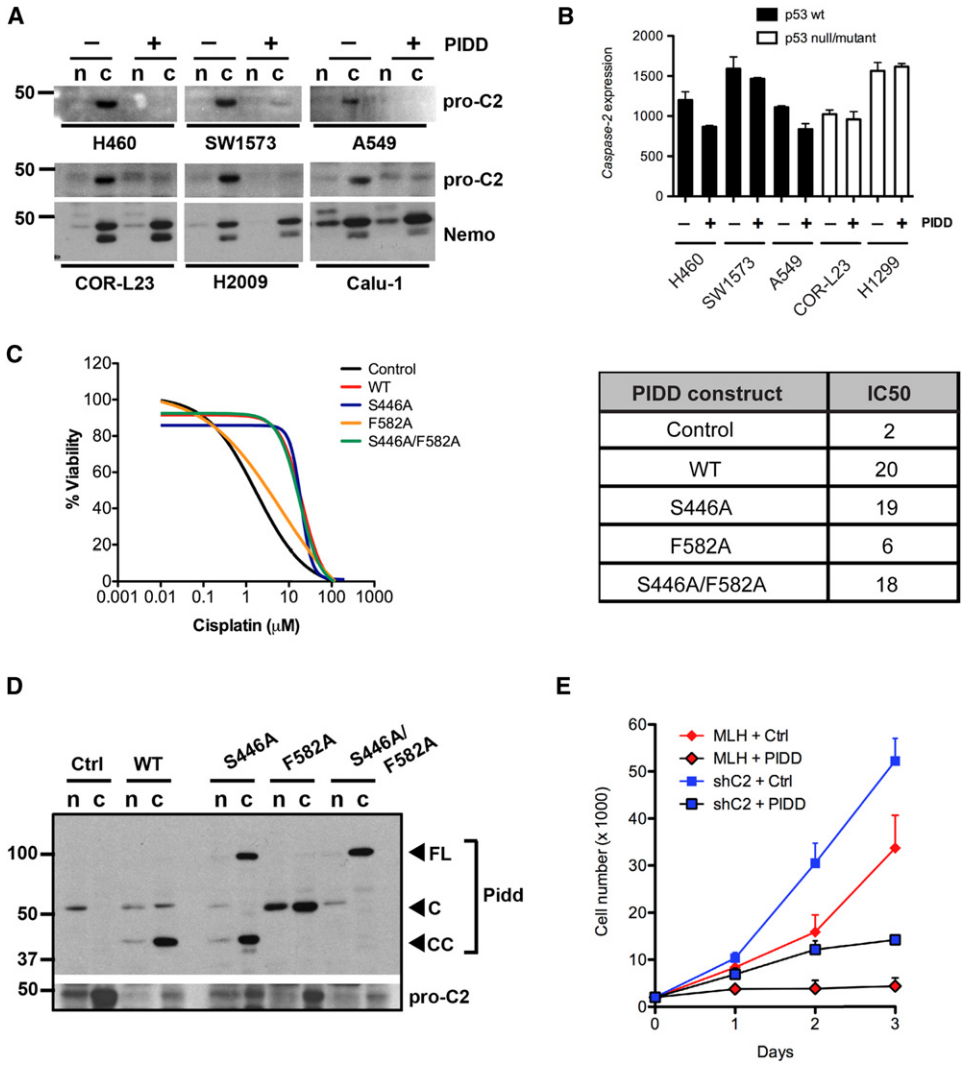

Figure 2. PIDD-Induced Growth Arrest and Cisplatin Resistance Depend on Caspase-2

(A) Immunoblot for pro-Caspase-2 in *p53* wild-type lines (top) with loading control in Figure 1E; *p53* null/mutant lines (bottom) with Nemo as cytoplasmic loading control.

(B) *Caspase-2* levels analyzed by real time RT-PCR and normalized to *actin,* n = 3.

(C) Cell viability assays performed with MSCV-control, PIDD, or PIDD point mutants (S446A, F582A, and S446A/F582A) stably expressed in H460 cells, n = 3. IC_{50} presented in table (μM, cisplatin).

(D) Immunoblot of n/c lysates from (C). Full-length (FL) and cleavage fragments of PIDD indicated by arrowheads.

(E) Growth rate of A549 cells stably expressing control (MLH) or Caspase-2 shRNAs (shC2) ± PIDD. Performed in triplicate; n = 2.

Error bars in all panels represent the mean ± SD. See also Figure S2.

of *CASP2* by p53 (Baptiste-Okoh et al., 2008) is not likely under these conditions since the reduction of pro-Caspase-2 by ectopic PIDD expression occurred independently of *p53* status (Figure 2A) and *CASP2* mRNA was not dramatically affected by PIDD expression (Figure 2B). Previous studies have demonstrated that Caspase-2 cleavage is not required for its full activation (Baliga et al., 2004) and that cleavage does not necessarily imply activation (Bouchier-Hayes et al., 2009). These results are consistent, however, with previous studies demonstrating PIDD's ability to promote Caspase-2 activation. Importantly, PIDD expression did not increase cleavage of PARP or Caspase-3 (Figure 1E, Figure S1D, and data not shown), suggesting that PIDD expression does not promote apoptosis under these conditions.

Given that PIDD is autocatalytically cleaved into multiple fragments that have been implicated in a variety of responses to cellular stress, we sought to determine which fragment(s) contribute to cell-cycle arrest and drug resistance. Point mutant versions of PIDD were stably expressed in human lung cancer cells that generate PIDD-C (F582A), PIDD-CC (S446A), or full-length PIDD (S466A/F582A) as previously described (Tinel et al., 2007). Expression of both PIDD-CC and full-length PIDD

induced growth arrest and cisplatin resistance in *p53* wild-type cells similar to wild-type PIDD, but PIDD-C did not (Figures 2C and 2D and data not shown). This suggests that PIDD-C, involved in NF-κB-mediated survival signaling, is not required for cell-cycle arrest and drug resistance. Expression of PIDD-CC, which has been implicated in Caspase-2 activation, was sufficient to promote cell-cycle arrest and drug resistance. Moreover, growth arrest and drug resistance correlated with the level of Caspase-2 cleavage (Figure 2D and data not shown), suggesting that Caspase-2 activation may be an important determinant of PIDD-induced cell-cycle arrest and drug resistance. To test this directly, we infected cells with Caspase-2 short hairpin RNAs (shRNAs) or controls and subsequently infected them with PIDD or controls. Caspase-2 knockdown was incomplete, but enhanced cell growth rate compared to control cells, similar to recent studies implicating Caspase-2 as a tumor suppressor (Ho et al., 2009). Importantly, reducing Caspase-2 levels partially rescued the growth rate of cells expressing PIDD (Figure 2E), suggesting that Caspase-2 is required for PIDD-induced cell-cycle arrest.

The Caspase-2-PIDDosome Promotes Mdm2 Cleavage

We hypothesized that the Caspase-2-PIDDosome may act to increase p53 levels by inhibiting Mdm2, a key negative regulator of p53. To address this, we analyzed Mdm2 expression in three NSCLC lines with or without PIDD expression. Low levels of full-length Mdm2 (~90 kDa) were present in all lines and did not dramatically differ in control versus PIDD-expressing cells (Figure 3A). Strikingly, however, an ~60 kDa Mdm2 species (referred to hereafter as p60) was highly enriched in PIDD-expressing cells compared to controls in all lines examined (Figure 3A). The Mdm2 p60 product could represent an alternative splice variant or cleavage product of Mdm2. Mdm2 p60 was detected with an N-terminal antibody, whereas two independent C-terminal Mdm2 antibodies detected a 25–30 kDa fragment (Figure 3A and data not shown) but did not detect p60. Thus, p60 appeared to be an N-terminal fragment of Mdm2. Consistent with this, relative levels of p60 and p25 fragments correlated well in all cell lines examined. The N-terminal fragment of Mdm2 was detected in the nucleus and cytoplasm of PIDD-expressing cells, whereas the p25 C-terminal fragment was found exclusively in the cytoplasm (Figure 3A). The N-terminal region of Mdm2 contains a nuclear localization sequence and nuclear export signal, whereas the C-terminal region does not (Coutts et al., 2009), consistent with the hypothesis that Mdm2 is cleaved in the cytoplasm and the p60 fragment enters the nucleus.

Mdm2 contains a well-conserved caspase cleavage site, Asp-Val-Pro-Asp (DVPD), at which cleavage generates an ~60 kDa N-terminal product (Pochampally et al., 1998). This site is conserved among human, mouse, and hamster (Chen et al., 1997; Pochampally et al., 1998). Upon re-examination of Mdm2 orthologs with recently annotated sequence data, we found that the DVPD site is also conserved in zebrafish mdm2 (Figure 3B). Previous studies demonstrated that activation of a temperature-sensitive p53 leads to Mdm2 cleavage at DVPD via a Caspase-3-like activity (Pochampally et al., 1999). This suggested to us that Caspase-2 might be the p53-induced caspase responsible for Mdm2 cleavage.

To test whether Mdm2 is cleaved at the DVPD site by Caspase-2, we mutated D367 to alanine (D367A) or glutamic acid (D367E) with vectors containing full-length N-terminal Myc-tagged human Mdm2 (Zhang et al., 2003). We also generated a truncated Mdm2 p60 by introducing a STOP codon after the DVPD site. Full-length Mdm2 (WT), D367A, D367E, p60, or eGFP control vectors were transiently expressed in 293T cells, and nuclear and cytoplasmic fractions were immunoblotted with anti-Myc-tag antibodies. Expression of wild-type Mdm2 led to appearance of the full-length Mdm2 protein as well as low levels of p60 products (Figure 3C). Expression of D367A and D367E eliminated expression of the p60 products. Importantly, transiently expressed Mdm2 p60 migrated at the same size as the cleavage products that were present upon wild-type Mdm2 expression (Figure 3C). Since Mdm2 contains an internal alternative start codon at amino acid 50, two full-length and two cleavage products were present, migrating as a doublet. Similar results were observed using A549 cells (data not shown). These data suggest that Mdm2 is cleaved at D367, generating a p60 protein doublet consistent with previous studies (Pochampally et al., 1998).

To test whether PIDD expression can promote Mdm2 cleavage, we expressed PIDD in 293T cells in the presence or absence of Myc-tagged Mdm2. PIDD expression caused a decrease in full-length Mdm2 and an increase in cleaved Mdm2, enhancing the ratio of cleaved to full-length Mdm2 (Figure 3D). Expression of PIDD and RAIDD are known to promote formation of the PIDDosome and subsequent Caspase-2 activation (Kitevska et al., 2009). If the Caspase-2-PIDDosome was responsible for Mdm2 cleavage, then expression of RAIDD might also promote Mdm2 cleavage. Indeed, expression of RAIDD was sufficient to promote cleavage of wild-type, but not point mutant D367A Mdm2 (Figure 3E), whereas Nemo did not promote Mdm2 cleavage (Figure S3). We next tested whether activated Caspase-2 could promote Mdm2 cleavage. Expression vectors for truncated constitutively-active (C2) or catalytically dead (C320A) Caspase-2 (Guha et al., 2010) were cotransfected with wild-type or D367A Mdm2. Expression of Caspase-2, but not C320A, led to a striking disappearance of full-length Mdm2 and the generation of cleaved Mdm2 p60 (Figure 3F). Mutation of D367 to alanine completely abolished Mdm2 cleavage. Together, these data are fully consistent with a model in which formation of the Caspase-2-PIDDosome promotes Mdm2 cleavage.

Caspase-2 Cleaves Mdm2 In Vitro

Given that Caspase-2 could activate another caspase (such as Caspase-3) responsible for Mdm2 cleavage, we tested directly whether recombinant Caspase-2 could cleave Mdm2. Wild-type or D367A Mdm2 were transiently expressed in 293T cells followed by immunoprecipitation (IP) with anti-Myc-tag antibodies. The Mdm2 IPs were incubated alone or with recombinant Caspase-2 (C2) or Caspase-3 (C3) and were then subjected to immunoblotting with Mdm2 N-terminal or C-terminal antibodies. Full-length Mdm2 (~p90) was entirely absent in the reactions with Caspase-2, and Mdm2 was partially cleaved by Caspase-3 as previously described (Figure 4A). In the presence of both caspases, we detected increased p60 fragments

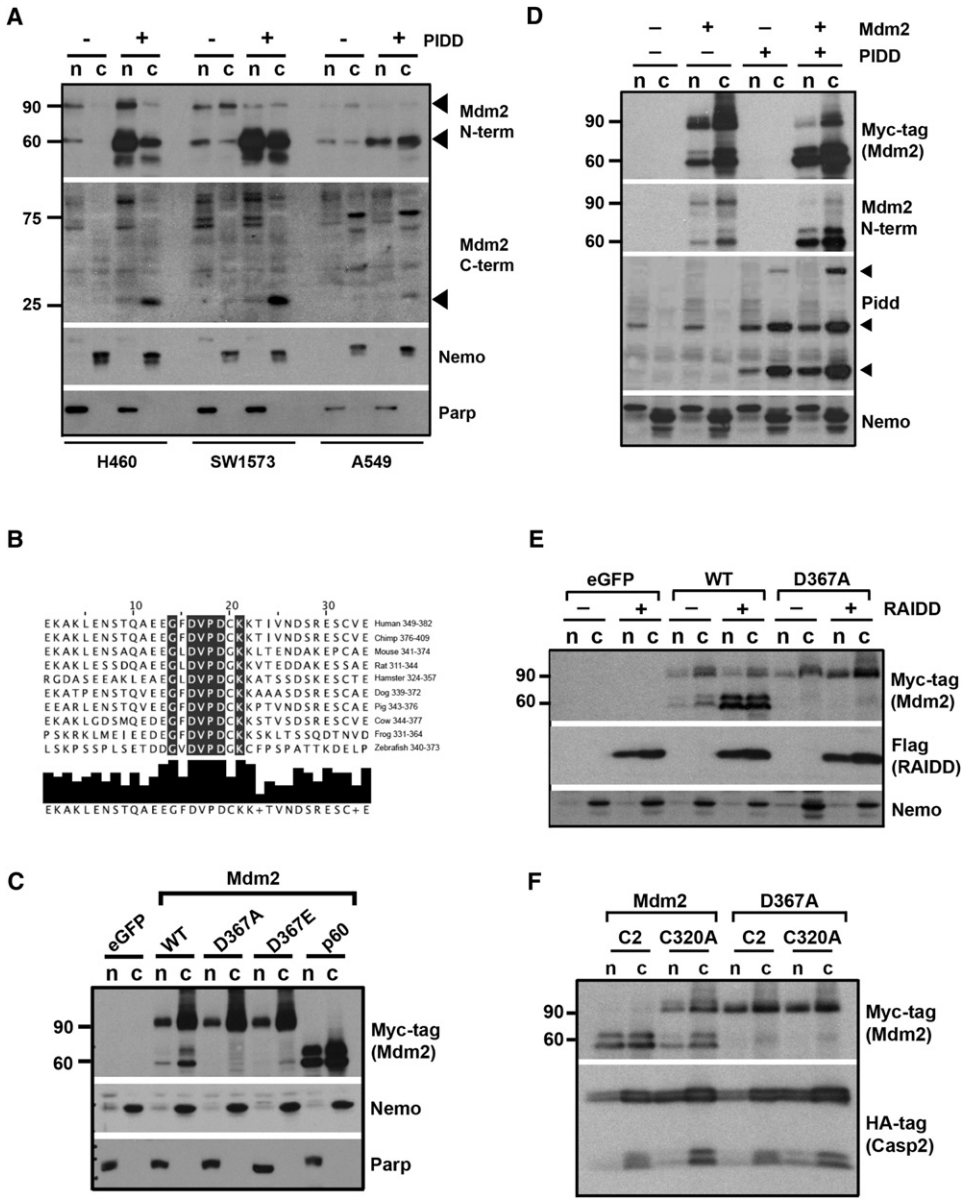

Figure 3. The Caspase-2-PIDDosome Promotes Mdm2 Cleavage

(A) Immunoblot of n/c lysates from control or PIDD-expressing NSCLC cell lines for Mdm2 expression.

(B) Sequence conservation of Mdm2 cleavage site, DVPD, among vertebrate species. Conserved residues are highlighted. Bottom plot shows consensus residues and degree of conservation at aligned sites.

(C) 293T cells transfected with eGFP control, myc-tagged Mdm2 (WT), point mutant Mdm2 (D367A), (D367E) or truncated Mdm2 (p60).

(D) Immunoblot of n/c fractions from 293T cells transiently expressing control or MSCV-PIDD ± myc-tagged Mdm2.

(E) Immunoblot of n/c fractions from 293T cells expressing control or Flag-tagged RAIDD with wild-type (WT) or D367A Mdm2.

(F) Immunoblot of n/c fractions from 293T cells expressing truncated HA-tagged active or inactive (C320A) Caspase-2 with wild-type or D367A Mdm2.

See also Figure S3.

using N-terminal antibodies and increased p30 fragments using C-terminal antibodies (Figure 4A). Cleavage probably occurred at the DVPD site, as the D367A mutant was not cleaved by either caspase. Recombinant Caspase-2 and -3 were also able to cleave recombinant Mdm2 (Figure 4B), demonstrating that both Caspase-2 and -3 can cleave Mdm2 in vitro. Importantly, given that Caspase-3 activity is not detectable in cells under the growth arrest conditions induced by PIDD in our experimental conditions, these results suggest that activated Caspase-2 directly cleaves Mdm2 after PIDDosome activation.

Low levels of exogenous Mdm2 p60 were present in 293T cells without addition of exogenous Caspase-2 (see Figure 3C, WT lane), so it was possible that basal Caspase-2 activity was present in these cells. Thus, we cotransfected Mdm2 with

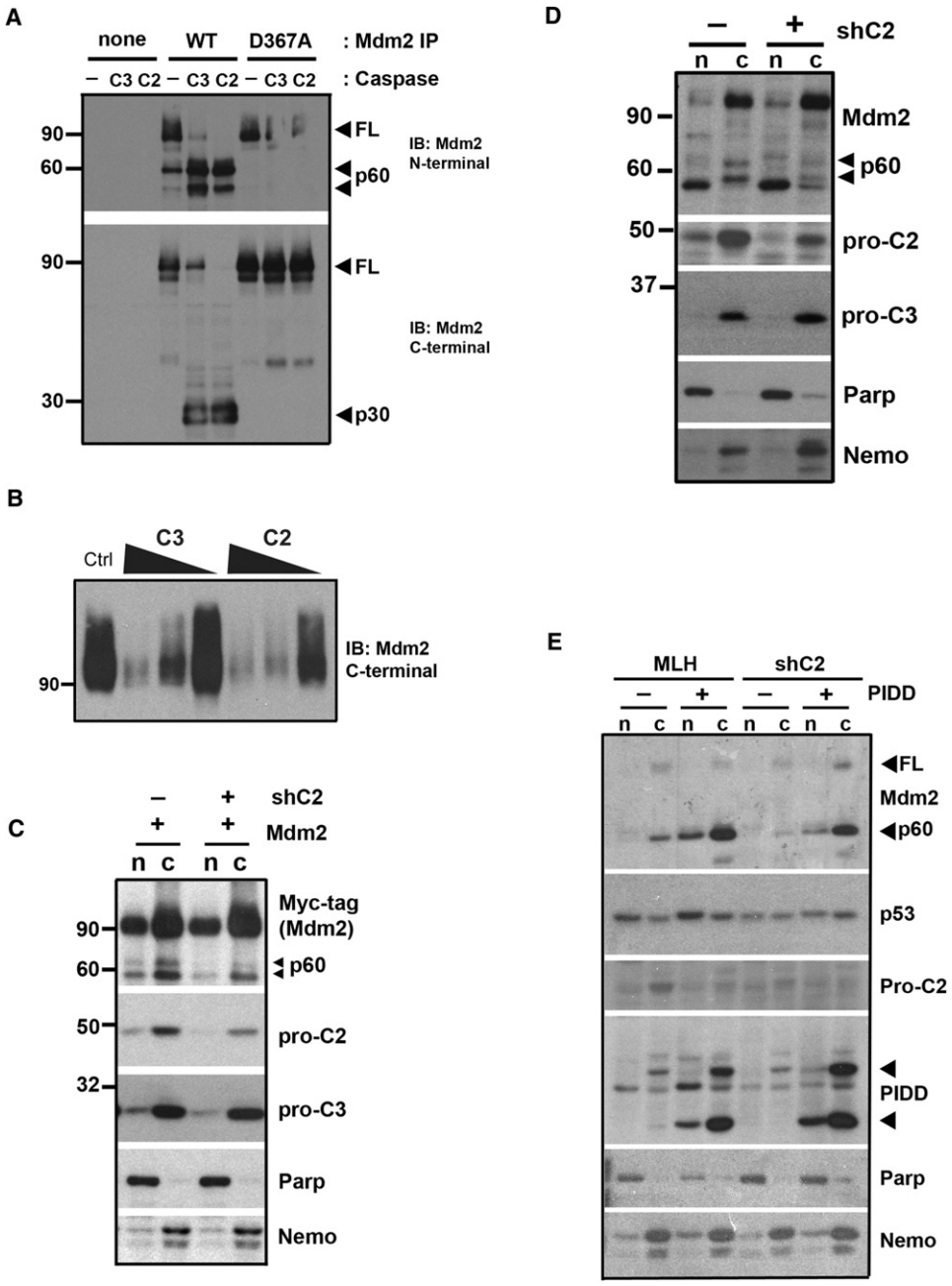

Figure 4. Caspase-2 Cleaves Mdm2 In Vitro

(A) IPs from 239T cells expressing control (none), wild-type (WT), or D367A Mdm2 incubated ± recombinant human Caspase-2 (C2) or Caspase-3 (C3). Immunoblot for Mdm2 (N-terminal and C-terminal antibodies) with full-length (FL) and cleavage fragments indicated by arrows.

(B) Immunoblot for Mdm2 (C-terminal) from recombinant Mdm2 incubated ± 5-fold serial dilutions (black arrows) in the presence or absence (ctrl) of recombinant Caspase-2 (C2) or Caspase-3 (C3).

(C) Immunoblot of n/c fractions from 293T cells transiently expressing myc-tagged Mdm2 ± MSCV-shCasp2. Mdm2 p60 fragments indicated by double arrowheads.

(D) Immunoblot of n/c fractions from A549 cells stably expressing MSCV-shCasp2 or vector control. Parp/Nemo immunoblots for n/c loading controls, respectively.

(E) Immunoblot of n/c lysates from A549 cells ± vector (MLH) or shC2, ± PIDD or vector control.

retroviral vectors carrying control or Caspase-2 shRNAs and examined Mdm2 expression. Caspase-2 knockdown was incomplete but significantly reduced the level of Mdm2 p60 (Figure 4C). To test whether Caspase-2 knockdown was sufficient to reduce cleavage of endogenous Mdm2, we stably infected A549 cells with retroviral vectors carrying Caspase-2

shRNAs or controls. Again, Caspase-2 knockdown was not complete, but reduction of Caspase-2 significantly inhibited cleavage of endogenous Mdm2 (Figure 4D). Expression of Caspase-2 shRNAs had no effect on pro-Caspase-3, -6, -8, or -9 levels (Figures 4C and 4D and data not shown). These data demonstrate that Caspase-2 cleaves Mdm2 in vitro and in human cancer cells. Furthermore, knockdown of Caspase-2 in PIDD-expressing cells reduced Mdm2 cleavage and nuclear p53, suggesting that Caspase-2 is required for Mdm2 cleavage and subsequent p53 accumulation (Figure 4E).

Cleaved Mdm2 Binds p53 and Promotes p53 Stabilization

The N terminus of Mdm2 harbors a well-characterized p53 binding domain (Chen et al., 1993). Upon cleavage at D367, the p53-binding domain is dissociated from the C-terminal ubiquitin-conjugating RING finger domain. Truncated forms of Mdm2 fail to target p53 for degradation and consequently lead to elevated p53 levels (Honda and Yasuda, 2000; Kubbutat et al., 1997; Pochampally et al., 1999). To determine whether Mdm2 p60 binds p53 in cells, we immunoprecipitated p53 from A549 cells expressing PIDD or vector control. As expected, PIDD-expressing cells had increased levels of p53 and Mdm2 cleavage compared to controls (Figure 5A, left). Western blotting of the p53 IPs with antibodies to Mdm2 (N-terminal and C-terminal) revealed that full-length and Mdm2 p60 were both bound to p53 in the presence of PIDD and that p60 was bound at higher levels than full-length Mdm2 (Figure 5A, right). Both antibodies revealed that significantly less full-length Mdm2 was bound to p53 in PIDD-expressing cells compared to control cells.

Because Mdm2 p60 lacks the RING domain, it should fail to promote p53 modifications such as ubiquitination, sumoylation, and neddylation. Loss of the RING finger domain may also contribute to increased Mdm2 p60 stability due to decreased autoubiquitination (Honda and Yasuda, 2000). To determine the effects of Mdm2 p60 on p53, we expressed wild-type (WT), noncleavable (D367A), RING finger domain mutant (C464A), and truncated Mdm2 (p60) in 293T cells and analyzed p53 levels. Wild-type and noncleavable Mdm2 caused a dramatic increase in p53 modifications (Figure 5B), whereas Mdm2 C464A (Figure S4A) and Mdm2 p60 (Figure 5B) did not. We tested whether Mdm2 p60 could compete for interaction with p53 and inhibit p53 modification by full-length Mdm2. Each Mdm2 construct was expressed alone (WT, D367A, or p60) or in combination with p60 in 293T cells. Coexpression of Mdm2 p60 with either wild-type or D367A Mdm2 dramatically reduced p53 modifications (Figure 5B). In *p53* wild-type U2OS cells, exogenous expression of wild-type and D367A Mdm2 led to slightly reduced p53 levels, whereas Mdm2 p60 expression caused a significant increase in p53 levels (Figure 5C). Increased p53 levels in the presence of Mdm2 p60 were also associated with a reduction in p53 modifications (Figure S4B). Together, these data suggest that the Mdm2 p60 fragment promotes the stabilization of p53 by reducing p53 modifications, most likely ubiquitination and subsequent proteasomal-mediated degradation.

To further examine whether Mdm2 cleavage inhibits p53 modifications, we coexpressed either constitutively active (Casp2) or catalytically dead (C320A) Caspase-2 along with wild-type Mdm2 in 293T cells. Consistent with previous results, p53 modifications were completely inhibited by expression of active Caspase-2 but not by catalytically dead Caspase-2 (Figure 5D) or Nemo (see Figure S3). Similar results were obtained in U2OS cells (data not shown). Expression of RAIDD, which promotes Mdm2 cleavage (Figure 3E), also inhibited p53 modification in the presence of wild-type but not D367A Mdm2 (Figure S4C). These results suggest that activation of the Caspase-2-PIDDosome leads to Mdm2 cleavage by Caspase-2, thereby inhibiting Mdm2 and promoting p53 stability.

Caspase-2-PIDDosome Cleaves Mdm2 in Response to DNA Damage

Given that p53 induces *PIDD*, which activates Caspase-2 and promotes Mdm2 cleavage, we reasoned that p53 activation should promote Mdm2 cleavage in response to DNA damage. We treated U2OS osteosarcoma cells with increasing doses of doxorubicin (dox) and analyzed Mdm2 and p53 levels. Dox treatment led to increased total Mdm2 levels with corresponding increases in cleaved Mdm2 that were maximal at 0.5 μM and diminished at higher doses. Levels of p53 also peaked at 0.5 μM (Figure S5A). To assess the role of Caspase-2 in Mdm2 cleavage, we infected *p53* wild-type U2OS and A549 cells with retroviral vectors carrying Caspase-2 or control shRNAs and then damaged cells with dox. In both cell types, dox treatment caused Mdm2 cleavage that increased with damage (0–0.5 μM) (Figures 6A and 6B). Caspase-2 knockdown did not affect pro-Caspase-3 levels but did significantly reduce cleaved Mdm2 at the basal level and upon damage, suggesting that the Mdm2 cleavage products are generated in a Caspase-2-dependent manner (Figures 6A and 6B).

To determine whether the Caspase-2-PIDDosome was required for Mdm2 cleavage, we tested whether inhibition of *PIDD* or *RAIDD* impacted Mdm2 cleavage upon DNA damage. *PIDD* and *RAIDD* knockdown in U2OS cells did not affect *Caspase-3* levels (Figures 6C and 6D). Cells were then damaged with 0.5 μM of dox, a concentration that induces *PIDD* expression and Mdm2 cleavage (Figures S5A and S5B), and Mdm2 levels were assessed in cytoplasmic fractions by western blotting. Importantly, inhibition of *PIDD* or *RAIDD* had no effect on pro-Caspase-3, but resulted in a striking reduction in Mdm2 cleavage compared to control small interfering RNAs (siRNAs) (Figure 6E). Finally, we compared Mdm2 cleavage in the presence or absence of siRNAs to Caspase-2 or -3. Knockdown of Caspase-2, but not Caspase-3, significantly reduced Mdm2 p60 products (Figure 6F). Treatment with the double-strand break-inducing agent, neocarzinostatin, also caused Mdm2 cleavage, which was abolished by Caspase-2-PIDDosome inhibition (Figure S5C). These data demonstrate that DNA damage activates the Caspase-2-PIDDosome, leading to Caspase-2-mediated cleavage and inhibition of Mdm2.

The Caspase-2-PIDDosome Impacts p53 Dynamics during the DNA Damage Response

Inhibition of Mdm2 cleavage would be predicted to result in increased total Mdm2 and decreased p53 levels. To test this, we knocked down *Caspase-2* or *PIDD* and damaged cells with

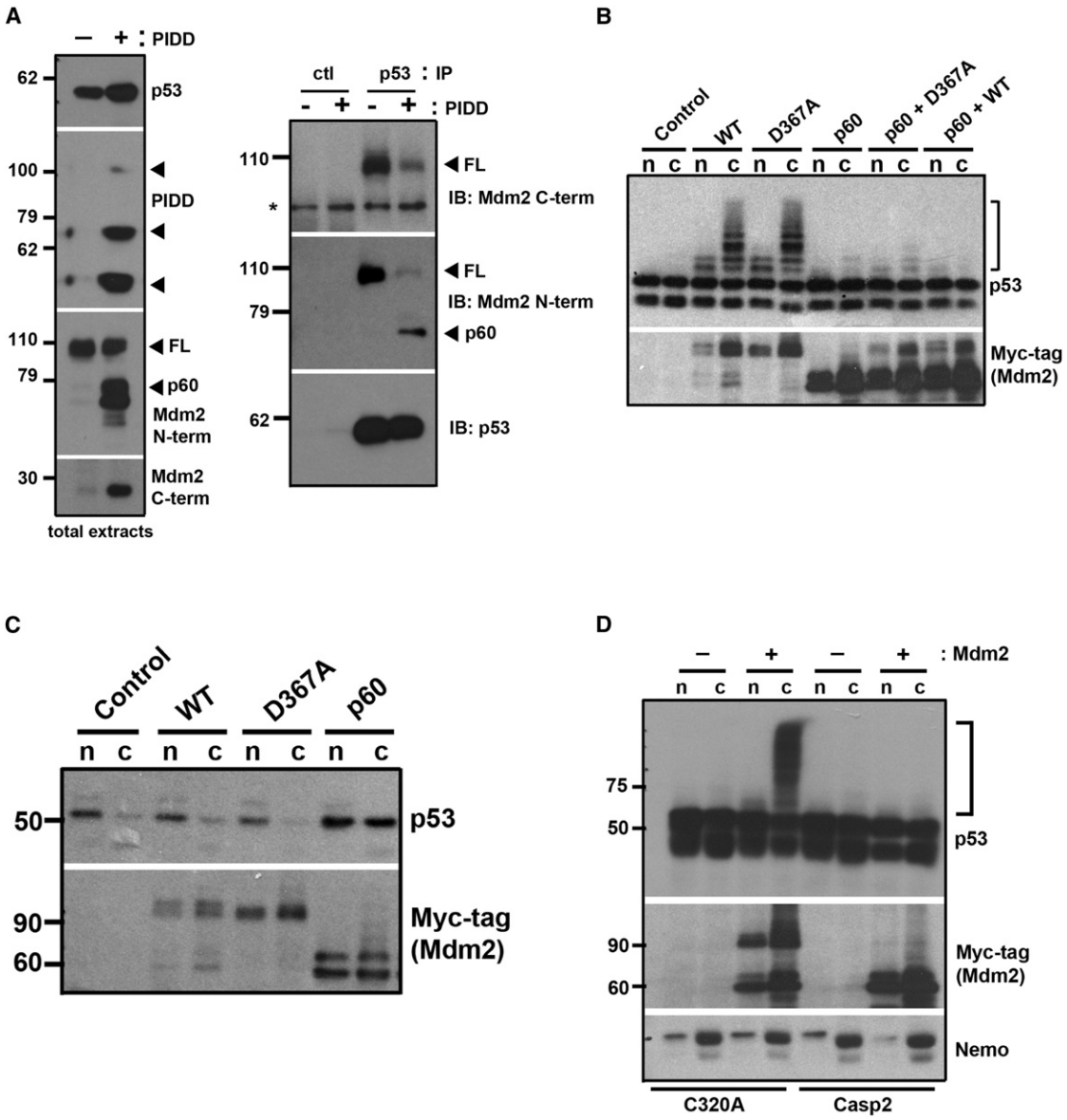

Figure 5. Cleaved Mdm2 Binds p53 and Promotes p53 Stabilization

(A) Left: Immunoblot of total extracts from control or PIDD-expressing A549 cells. Right: Control or p53 IPs blotted for Mdm2 (C-terminal and N-terminal) or p53. Asterisk (*) indicates nonspecific band.

(B) Immunoblot of n/c fractions from 293T cells transiently expressing control, wild-type (WT), point mutant (D367A), truncated Mdm2 (p60), or indicated combinations. Bracket indicates p53 modifications.

(C) Same as in (B), except in U2OS cells.

(D) Immunoblot of n/c fractions from 293T cells transiently expressing truncated active (Casp2) or catalytically dead (C320A) Caspase-2 ± Mdm2.

See also Figure S4.

dox. As predicted, p53 levels were slightly reduced at the basal level upon *Caspase-2* and *PIDD* knockdown (Figures 7A and 7B). Upon DNA damage, p53 levels recovered, and subsequently peaked earlier than control cells (e.g., 20 hr), followed by a dramatic decline in levels at 26 hr. This suggests that Mdm2 cleavage is not required for the initial accumulation of p53, but appears to impact the maintenance of p53 levels after DNA damage.

To assess the impact of the Caspase-2-PIDDosome on the recovery of cells after DNA damage, we treated cells with dox for 8 hr, washed and allowed them to recover. In control cells, p53 levels peaked by 24 hr. In cells with *Caspase-2* or *PIDD* knockdown, p53 levels were induced to a similar extent, but peaked earlier and declined prematurely after 32 hr (Figures 7A–7C and Figure S6A and S6B). Similar results were obtained in cells synchronized with hydroxyurea (data not shown).

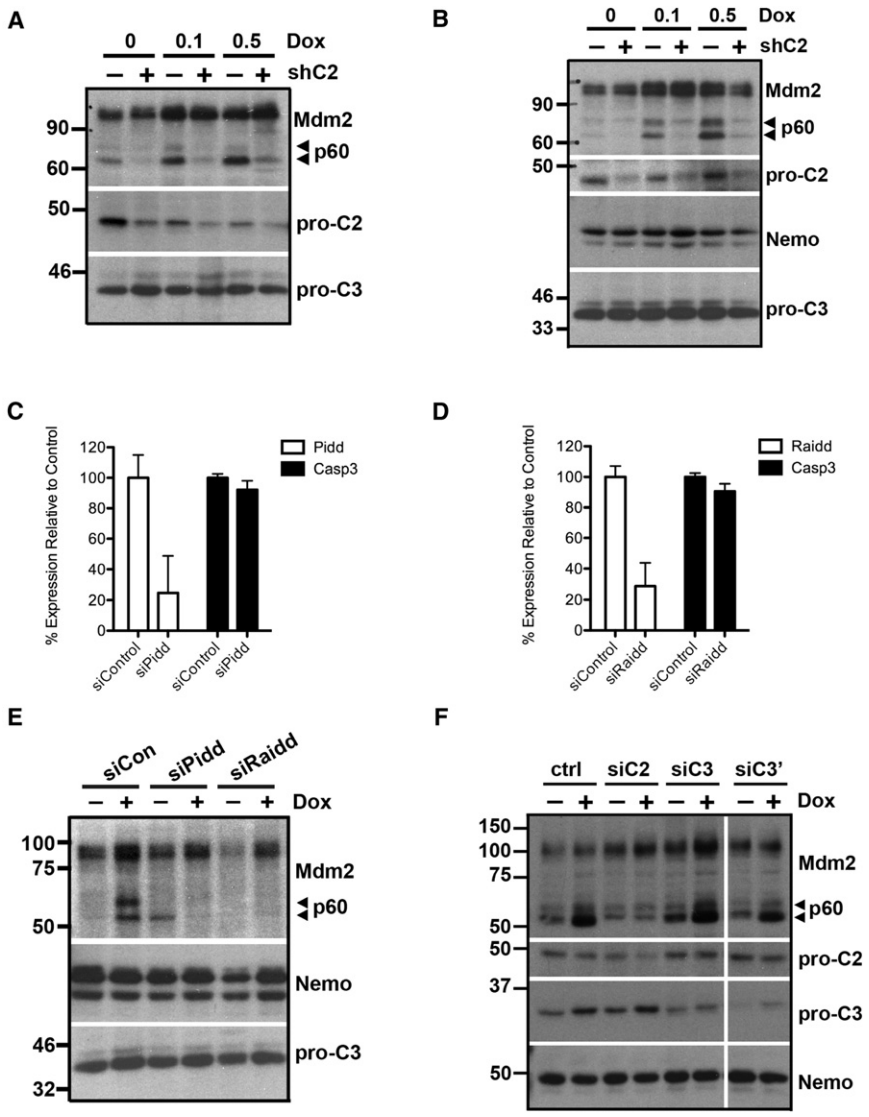

Figure 6. Caspase-2-PIDDosome Cleaves Mdm2 in Response to DNA Damage

(A) Immunoblot with cytoplasmic fractions from A549 cells treated with vehicle, 0.1, or 0.5 μM doxorubicin (Dox) ± MSCV-shCasp2 (shC2).

(B) Same as in (A), except in U2OS cells.

(C and D) Real time RT-PCR for human *PIDD* (C) or *RAIDD* (D) normalized to *ACTIN*, and relative to siRNA controls. Error bars represent the mean ± SD.

(E) Immunoblot of cytoplasmic lysates from U2OS cells treated ± 500 nM Dox for 24 hr. Nemo and pro-Casp3 immunoblot (controls).

(F) Same as in (E) with total cell lysates, with siRNAs to control (ctrl), Caspase-2 (siC2), or two different siRNAs to Caspase-3 (siC3, siC3′).

See also Figure S5.

Together, this suggests that the Caspase-2-PIDDosome is an important factor in maintaining p53 levels and regulating p53 dynamics after DNA damage.

Because PIDD expression promoted resistance to DNA damage in *p53* wild-type cells (Figure 1C), we sought to determine whether inhibition of PIDD would sensitize to DNA damage. We treated cells with control or *PIDD* siRNAs and measured apoptosis by flow cytometry after dox treatment. *PIDD* inhibition resulted in a significant increase in the percentage of apoptotic and dead cells compared to controls (Figure 7D). Together, these data suggest that Mdm2 cleavage by the Caspase-2-PIDDosome establishes a positive feedback loop induced by p53 that reinforces p53 stability and activity after DNA damage (Figure 7E).

DISCUSSION

Here, we show that activation of the Caspase-2-PIDDosome promotes cleavage of Mdm2. Caspase-2 directly cleaves Mdm2 at a conserved $DVPD_{367}$ site, leading to separation of the p53 binding domain and the RING finger responsible for p53 ubiquitination. As a result, Mdm2 cleavage inhibits its E3 ubiquitin ligase activity, leading to increased p53 levels and activity. We show that Mdm2 cleavage in human lung cancer cells promotes p53-dependent cell-cycle arrest and subsequent drug resistance. Furthermore, Mdm2 cleavage by the Caspase-2-PIDDosome occurs in response to DNA damage and contributes to the maintenance of p53 levels. Together, p53 activation of the Caspase-2-PIDDosome establishes a positive feedback loop that promotes p53 stability and activity after DNA damage (Figure 7E).

Previous studies showed that Mdm2 is cleaved by a Caspase-3-like activity under apoptotic and nonapoptoptic, growth arrest conditions (Chen et al., 1997; Erhardt et al., 1997; Pochampally et al., 1998, 1999). The caspase responsible for Mdm2 cleavage was p53 inducible (Pochampally et al., 1999) and distinct from Caspases-1, -3, -6, -7, and -8 (Erhardt et al., 1997; Pochampally et al., 1998, 1999). Thus, the identity of the caspase that directly cleaved Mdm2 and its mechanism of induction by p53 remained unknown. Our studies resolve these issues by demonstrating that (1) Caspase-2 directly cleaves Mdm2 and (2) the mechanism of Caspase-2 activation is due to p53-mediated induction of PIDD.

Very few Caspase-2 cleavage targets are known, making its biological role elusive. Interestingly, the Caspase-2 cleavage site identified here in Mdm2 (DVPD) is highly conserved among vertebrates and similar to the known Caspase-2 cleavage site, ESPD, of Golgin-160 (Mancini et al., 2000). Although studied here in the context of DNA damage and p53 activation, we speculate that this pathway may be important for p53 regulation more broadly. Recent studies by Ho et al. (2009) have implicated Caspase-2 as a tumor suppressor, and the authors noted that p53

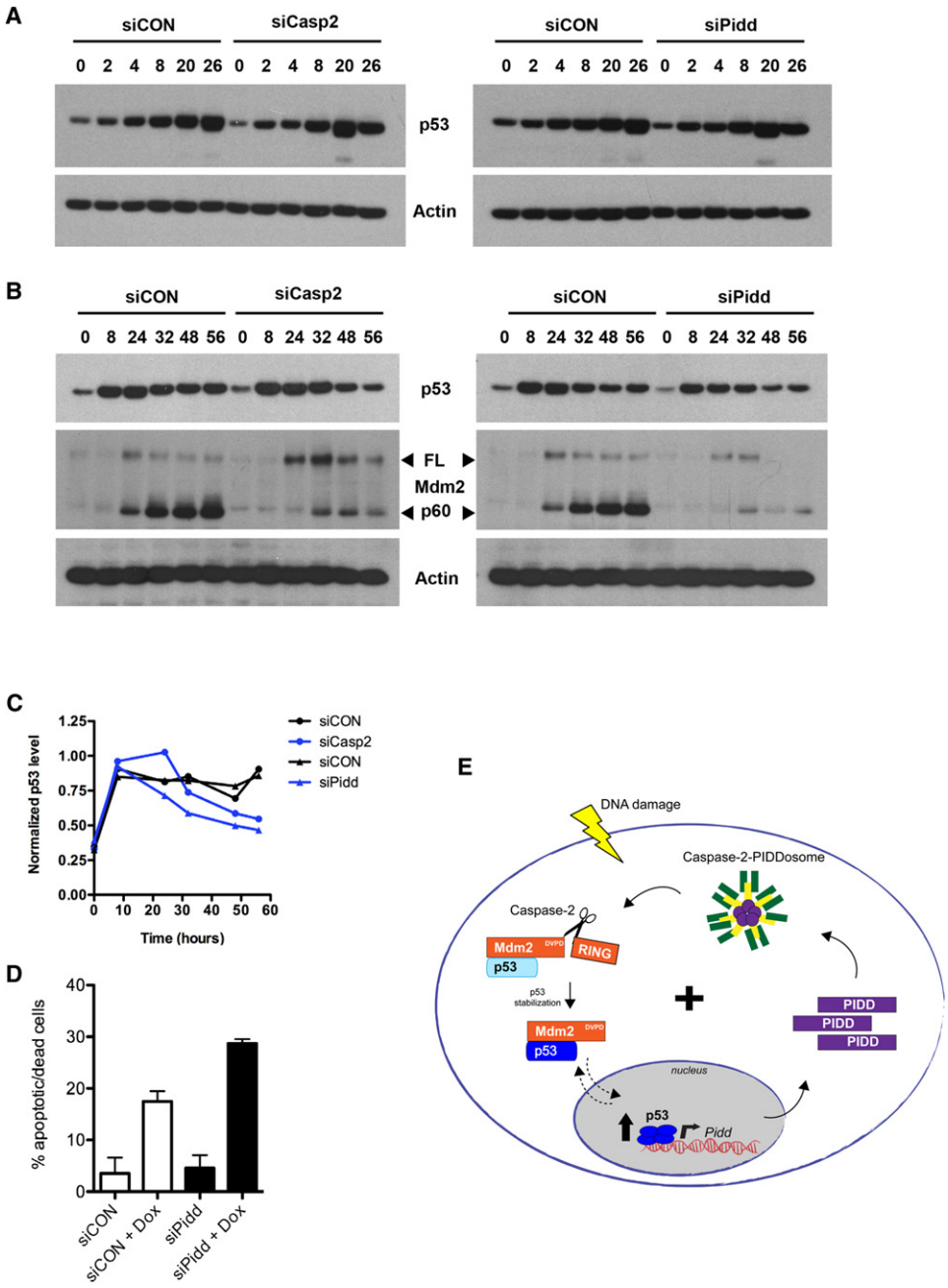

Figure 7. The Caspase-2-PIDDosome Regulates p53 Dynamics in Response to DNA Damage

(A) Immunoblot with total lysates from U2OS cells transfected with siControl (siCON) versus siCaspase-2 (left) or siPidd (right) treated with 0.5 μM Dox and harvested after the indicated hours.

(B) Same as in (A), except cells were washed after 8 hr damage and analyzed at later time points.

(C) Quantitation of p53 levels relative to ACTIN in (B).

(D) Apoptotic/dead cells measured by flow cytometry for Annexin-V in U2OS cells expressing siCON or siPidd cells treated ± Dox. Error bars represent the mean ± SD.

(E) Model of p53-induced positive feedback loop. Activation of p53 (here, via DNA damage) induces expression of the p53 target gene, *PIDD*. Increased PIDD expression promotes Caspase-2-PIDDosome formation, leading to activation of Caspase-2 as previously shown. Full-length Mdm2, an E3 ubiquitin ligase, can promote ubiquitination and degradation of p53 (unstable p53, light blue). Activated Caspase-2 cleaves Mdm2 at amino acids DVPD, separating the N-terminal p53-binding domain from the RING domain. Cleaved Mdm2 can bind p53 but cannot promote its degradation (stabilized p53, dark blue)—ultimately reinforcing p53 levels in a positive feedback loop.

See also Figure S6.

activity is reduced in *caspase-2* null MEFs. This phenotype is consistent with our model in which Caspase-2 depletion reduces Mdm2 cleavage, thus permitting increased expression of full-length Mdm2 and enhanced degradation of p53. Consistent with Ho et al. (2009), we observe that Caspase-2 knockdown accelerates cell growth and results in reduced p53 and p21 levels (data not shown).

In contrast to our findings, previous studies implicated Caspase-2 in heat shock-induced apoptosis and failed to detect Caspase-2 activation upon other types of genotoxic stress (Tu et al., 2006). Because these studies were performed in T cells and splenocytes, it remains possible that cell type-specific differences explain this discrepancy. We initially tested the effects of PIDD in response to cisplatin in lung cancer cells, but began to use U2OS cells for their ease of manipulation for siRNA and complementary DNA transfections. We tested doxorubicin on U2OS cells, as it is a common therapeutic agent for osteosarcoma and subsequently confirmed that doxorubicin and neocarzinostatin, a double-strand break inducer, also affect Mdm2 cleavage in lung cancer cells (Figure 6A and Figure S5C).

Mdm2 contains other potential caspase cleavage sites located N-terminal to the DVPD site. Because Caspase-3 can cleave Mdm2 at high levels, it is possible that Caspase-2 initially cleaves Mdm2 under low levels of DNA damage, while excessive damage activates Caspase-3, leading to complete degradation of Mdm2 via additional cleavage sites. Recent studies have identified a mechanism of Mdm2 degradation involving phosphorylation by casein kinase 1 and subsequent β-TRCP-mediated destruction (Inuzuka et al., 2010). The levels of DNA damage used in our experiments promote growth arrest and did not lead to complete degradation of Mdm2. However, upon higher levels of damage, we observed a reduction in full-length and cleaved Mdm2 (Figure S5A). Therefore, we hypothesize that the mode of Mdm2 regulation identified here is particularly important under reparable levels of DNA damage.

Mdm2 interaction with p53 has been shown to inhibit p53-transcriptional activity in vitro, but genetically engineered mouse models have led to uncertainty about the in vivo relevance of these findings (Itahana et al., 2007). Itahana et al. demonstrated that *Mdm2* C462A mutant mice, in which Mdm2 lacks ubiquitin-conjugation function but retains p53-binding capacity, are embryonic lethal, similar to *Mdm2* null mice. Embryonic lethality of *Mdm2* C462A mice is rescued by p53 loss indicating that Mdm2 binding to p53 is not sufficient to inhibit p53 in vivo (Itahana et al., 2007). Therefore, it may not be surprising that in the presence of Mdm2 p60 we find stabilized p53 that appears to be transcriptionally active and capable of inducing *p21* and other p53 target genes (data not shown). How Mdm2 cleavage ultimately impacts the transcriptional program induced by p53 is an interesting avenue of further investigation.

Mdm2 cleavage in human lung cancer cells led to p21 induction and cell cycle arrest. We hypothesize that this mechanism of transient Mdm2 inhibition could serve to protect *p53* wild-type tumors treated with chemotherapy, if enhanced p53 preferentially induces cell-cycle arrest and/or DNA damage repair. Consistent with this hypothesis, we recently observed that *Pidd* is more highly induced in cisplatin-resistant tumors compared to naive tumors in response to chemotherapy in vivo (Oliver et al., 2010), suggesting that p53 may promote arrest or repair in this context. Given that context-specific posttranslational modifications of p53 may also regulate its activity, it remains possible that p53 stability may promote functions other than growth arrest such as apoptosis, senescence, or autophagy under different cellular conditions.

Mdm2 can bind a number of important proteins via its N-terminal and central acidic domains, such as Rb and ARF, and can regulate the activity of other proteins by ubiquitination (Coutts et al., 2009). Therefore, Mdm2 cleavage by Caspase-2 may have important consequences for the regulation of a variety of p53-dependent and -independent processes. Importantly, Mdm2 and the Mdm2 homolog, MdmX, bind through their C-terminal RING domains (Tanimura et al., 1999). Thus, Mdm2 cleavage is predicted to abolish interaction with MdmX. The DVPD cleavage site in Mdm2 is also conserved in MdmX (Pochampally et al., 1998), but we do not detect MdmX cleavage under these conditions (Figure S5D). MdmX is detected largely in the nucleus of human lung cancer cell lines, which may preclude efficient interaction with Caspase-2 in the cytoplasm (Figure S5D). In either case, cleavage of MdmX and/or Mdm2 at DVPD would be expected to abolish Mdm2/MdmX heterodimer formation (Wade et al., 2010) and prevent Mdm2-mediated ubiquitination of p53. While our studies did not preclude that Mdm2 cleavage also inhibits the sumoylation and neddylation of p53, ubiquitination of p53 is known to control its levels, whereas sumoylation and neddylation have not been implicated in p53 stability (Dai and Gu, 2010). Mdm2 has been shown to degrade MdmX upon DNA damage (de Graaf et al., 2003; Pan and Chen, 2003), suggesting that cleaved Mdm2 p60 could enhance MdmX levels and counter p53 activity. Inhibition of the Caspase-2-PIDDosome upon DNA damage did not appear to enhance MdmX degradation in the assays used here (data not shown).

Many p53 autoregulatory loops impinge on Mdm2 (Harris and Levine, 2005; Lu, 2010) and regulate Mdm2 by a variety of mechanisms, including interaction with MdmX, autoubiquitination, phosphorylation, and, here, cleavage (Wade et al., 2010). We observe that inhibition of the Caspase-2-PIDDosome does not prevent p53 induction upon DNA damage, but impacts the dynamics of p53 levels over time. During the past decade, it has become appreciated that p53 exhibits pulsatile dynamics in response to DNA damage (Batchelor et al., 2008; Lahav et al., 2004; Loewer et al., 2010). We speculate that the p53-Caspase-2-PIDDosome-Mdm2 pathway identified here may contribute to p53 pulses during DNA damage, by shutting down Mdm2 activity and re-establishing p53 activity. This positive feedback loop initiated by p53-induction of *PIDD* may thus serve as an important counterbalance to p53 induction of *Mdm2*. Together, these findings highlight the complexity of the feedback loops dictating p53 response and undoubtedly contribute to the cell's ability to control p53 with exquisite sensitivity.

EXPERIMENTAL PROCEDURES

Cell Lines, Antibodies, Constructs, and Reagents

Human NSCLC lines were kindly provided by Jeffrey Settleman or obtained from ATCC. A427, A549, SW1573, H23, H1944, and H2009 cell lines were

maintained in DMEM. H460, COR-L23, and Calu-1 were cultured in RPMI. 293T, U2OS, HCT116 $p53^{+/+}$ and $p53^{-/-}$, and $Kras^{LA/+}$; $p53^{LSL/LSL}$; $ROSA26^{CreERT2}$ cells (provided by D. Feldser) were maintained in DMEM. For p53 restoration, KPR cells were treated with 250 nM hydroxytamoxifen (4-OHT, Sigma) or vehicle control (ethanol). Transient transfections were performed using Mirus with 2–10 μg DNA per 10 cm dish. For generation of viral supernatants, 293T cells were transfected with MSCV vectors, Gag/pol, and Env plasmids, and supernatants were harvested after 48–72 hr. Human cell lines were infected twice with retroviral supernatant at 1:1 (media: supernatant) with 1000X polybrene (8 μg/ml) and then selected for 2–3 days in puromycin. Antibodies, constructs and reagents are provided in the Supplemental Experimental Procedures.

siRNA

siRNAs were obtained from QIAGEN: AllStars negative siCONTROL (#1027286), human CRADD/RAIDD #2 (SI00056035), LRDD/PIDD as published in (Tinel and Tschopp, 2004), Caspase-2 #10 (SI00299551) and #11 (SI02625546), and Caspase-3 #2 (SI00062937) and #9 (SI03100041). U2OS cells were transfected with siRNAs (20 nM) in Opti-MEM with Mirus *Trans*IT-TKO transfection reagent according to manufacturer's instructions. After 24 hr, cells were damaged with doxorubicin and harvested after various time points for western blot as described. For knockdown validation, cells were harvested 30 hr after transfection. RNA was isolated and subjected to real time RT-PCR as described in the Supplemental Experimental Procedures.

Western Blotting

For nuclear and cytoplasmic fractionations, lysates were prepared as previously described (Oliver et al., 2010). Protein samples were separated via SDS-PAGE and blotted to a PVDF membrane. Membranes were blocked for 1 hr, followed by overnight incubation with primary antibodies at 4°C. Membranes were washed 6 × 5 min at room temperature. HRP-conjugated secondary antibodies (Jackson ImmunoResearch, 1:10,000) were incubated for 1 hr at room temperature. For detection, membranes were exposed to Western-Lightning ECL (Perkin-Elmer) and detected on Kodak film. Blots were stripped and reprobed for PARP and/or NEMO for nuclear and cytoplasmic controls, respectively.

Immunoprecipitations

Cells were lysed on ice for 10 min in a buffer containing 0.1% NP-40, 5 mM EDTA, 50 mM Tris (pH 8.0), and 150 mM NaCl, followed by three cycles of freezing and thawing. After centrifugation (4°C, 10 min, 16,000 g), the supernatants were precleared at 4°C on a rotating wheel for 45 min in the presence of 20 μl sepharose 6B (Sigma). After centrifugation (4°C, 1 min, 1900 g), a small fraction of supernatant was frozen for later analysis (cell extract), and the remaining fraction was incubated at 4°C on a rotating wheel, overnight, in the presence of 10 μl sepharose 6B, 10 μl protein G sepharose (GE Healthcare), and 0.5 μg of desired antibody. The IPs bound to protein G were washed three times in lysis buffer, prior to boiling in sample buffer containing DTT for analysis by western blot.

For the Mdm2 cleavage assay, the washed Mdm2 IPs bound to protein G were incubated with 0.5 units of recombinant Caspase-2 or Caspase-3 (Enzo Life Sciences, units specified by manufacturer) in a buffer containing 0.1% CHAPS, 20 mM HEPES (pH 7.2), 50 mM NaCl, 10 mM EDTA, 5% glycerol, and 10 mM DTT. After 45 min incubation at 37°C, samples were boiled in sample buffer containing DTT for analysis by western blot.

In Vitro Caspase Assay

For each reaction, 10 ng recombinant Mdm2 (Calbiochem, catalog number 444146) was added to buffer containing 0.1% CHAPS, 20 mM HEPES (pH 7.2), 50 mM NaCl, 10 mM EDTA, 5% glycerol, and 10 mM DTT. Mdm2 was incubated alone or in the presence of increasing amounts of recombinant Caspase-2 or Caspase-3 (0.02, 0.1, or 0.5 units, according to manufacturer's instructions). The samples were incubated for 45 min at 37°C and then terminated by boiling in sample buffer containing DTT. Samples were then loaded on gels for analysis by western blot.

SUPPLEMENTAL INFORMATION

Supplemental Information includes Supplemental Experimental Procedures and six figures and can be found with this article online at doi:10.1016/j.molcel.2011.06.012.

ACKNOWLEDGMENTS

We wish to dedicate this work to the memory of our friend, colleague and mentor, Dr. Jürg Tschopp, whose work established the foundation for our understanding of the PIDDosome. We are grateful to Mike Hemann and Nadya Dimitrova for helpful comments and critical reading of the manuscript, and to Anne Deconinck and Judy Teixeira for excellent administrative support. We thank A. Tinel for kindly providing PIDD and RAIDD constructs, M. Guha and D.C. Altieri for Caspase-2 constructs, D. Feldser for p53-restorable cell lines, Y. Xiong for pCMV-myc3-Mdm2, and G. Paradis for technical support. T.O. is an ASPET-Merck postdoctoral fellow and supported by a Ludwig Fund postdoctoral fellowship. E.M. was supported by a fellowship from the International Human Frontier Science Program Organization. T.J. is an Investigator of the Howard Hughes Medical Institute and a Daniel K. Ludwig Scholar.

This work was also supported in part by Cancer Center Support (core) grant P30-CA14051 (T.J.).

Received: February 28, 2011
Revised: May 11, 2011
Accepted: June 9, 2011
Published: July 7, 2011

REFERENCES

Baliga, B.C., Read, S.H., and Kumar, S. (2004). The biochemical mechanism of caspase-2 activation. Cell Death Differ. *11*, 1234–1241.

Baptiste-Okoh, N., Barsotti, A.M., and Prives, C. (2008). Caspase 2 is both required for p53-mediated apoptosis and downregulated by p53 in a p21-dependent manner. Cell Cycle *7*, 1133–1138.

Batchelor, E., Mock, C.S., Bhan, I., Loewer, A., and Lahav, G. (2008). Recurrent initiation: a mechanism for triggering p53 pulses in response to DNA damage. Mol. Cell *30*, 277–289.

Batchelor, E., Loewer, A., and Lahav, G. (2009). The ups and downs of p53: understanding protein dynamics in single cells. Nat. Rev. Cancer *9*, 371–377.

Bergeron, L., Perez, G.I., Macdonald, G., Shi, L., Sun, Y., Jurisicova, A., Varmuza, S., Latham, K.E., Flaws, J.A., Salter, J.C., et al. (1998). Defects in regulation of apoptosis in caspase-2-deficient mice. Genes Dev. *12*, 1304–1314.

Bouchier-Hayes, L., Oberst, A., McStay, G.P., Connell, S., Tait, S.W.G., Dillon, C.P., Flanagan, J.M., Beere, H.M., and Green, D.R. (2009). Characterization of cytoplasmic caspase-2 activation by induced proximity. Mol. Cell *35*, 830–840.

Chen, J., Marechal, V., and Levine, A.J. (1993). Mapping of the p53 and mdm-2 interaction domains. Mol. Cell. Biol. *13*, 4107–4114.

Chen, L., Marechal, V., Moreau, J., Levine, A.J., and Chen, J. (1997). Proteolytic cleavage of the mdm2 oncoprotein during apoptosis. J. Biol. Chem. *272*, 22966–22973.

Coutts, A.S., Adams, C.J., and La Thangue, N.B. (2009). p53 ubiquitination by Mdm2: a never ending tail? DNA Repair (Amst.) *8*, 483–490.

Dai, C., and Gu, W. (2010). p53 post-translational modification: deregulated in tumorigenesis. Trends Mol. Med. *16*, 528–536.

de Graaf, P., Little, N.A., Ramos, Y.F., Meulmeester, E., Letteboer, S.J., and Jochemsen, A.G. (2003). Hdmx protein stability is regulated by the ubiquitin ligase activity of Mdm2. J. Biol. Chem. *278*, 38315–38324.

Erhardt, P., Tomaselli, K.J., and Cooper, G.M. (1997). Identification of the MDM2 oncoprotein as a substrate for CPP32-like apoptotic proteases. J. Biol. Chem. *272*, 15049–15052.

Feldser, D.M., Kostova, K.K., Winslow, M.M., Taylor, S.E., Cashman, C., Whittaker, C.A., Sanchez-Rivera, F.J., Resnick, R., Bronson, R., Hemann, M.T., and Jacks, T. (2010). Stage-specific sensitivity to p53 restoration during lung cancer progression. Nature *468*, 572–575.

Guha, M., Xia, F., Raskett, C.M., and Altieri, D.C. (2010). Caspase 2-mediated tumor suppression involves survivin gene silencing. Oncogene *29*, 1280–1292.

Guo, Y., Srinivasula, S.M., Druilhe, A., Fernandes-Alnemri, T., and Alnemri, E.S. (2002). Caspase-2 induces apoptosis by releasing proapoptotic proteins from mitochondria. J. Biol. Chem. *277*, 13430–13437.

Hamstra, D.A., Bhojani, M.S., Griffin, L.B., Laxman, B., Ross, B.D., and Rehemtulla, A. (2006). Real-time evaluation of p53 oscillatory behavior in vivo using bioluminescent imaging. Cancer Res. *66*, 7482–7489.

Harris, S.L., and Levine, A.J. (2005). The p53 pathway: positive and negative feedback loops. Oncogene *24*, 2899–2908.

Haupt, Y., Maya, R., Kazaz, A., and Oren, M. (1997). Mdm2 promotes the rapid degradation of p53. Nature *387*, 296–299.

Ho, L.H., Taylor, R., Dorstyn, L., Cakouros, D., Bouillet, P., and Kumar, S. (2009). A tumor suppressor function for caspase-2. Proc. Natl. Acad. Sci. USA *106*, 5336–5341.

Honda, R., and Yasuda, H. (2000). Activity of MDM2, a ubiquitin ligase, toward p53 or itself is dependent on the RING finger domain of the ligase. Oncogene *19*, 1473–1476.

Horn, H.F., and Vousden, K.H. (2007). Coping with stress: multiple ways to activate p53. Oncogene *26*, 1306–1316.

Inuzuka, H., Tseng, A., Gao, D., Zhai, B., Zhang, Q., Shaik, S., Wan, L., Ang, X.L., Mock, C., Yin, H., et al. (2010). Phosphorylation by casein kinase I promotes the turnover of the Mdm2 oncoprotein via the SCF(beta-TRCP) ubiquitin ligase. Cancer Cell *18*, 147–159.

Itahana, K., Mao, H., Jin, A., Itahana, Y., Clegg, H.V., Lindström, M.S., Bhat, K.P., Godfrey, V.L., Evan, G.I., and Zhang, Y. (2007). Targeted inactivation of Mdm2 RING finger E3 ubiquitin ligase activity in the mouse reveals mechanistic insights into p53 regulation. Cancer Cell *12*, 355–366.

Janssens, S., Tinel, A., Lippens, S., and Tschopp, J. (2005). PIDD mediates NF-kappaB activation in response to DNA damage. Cell *123*, 1079–1092.

Jordan, J.J., Menendez, D., Inga, A., Noureddine, M., Bell, D.A., and Resnick, M.A. (2008). Noncanonical DNA motifs as transactivation targets by wild type and mutant p53. PLoS Genet. *4*, e1000104.

Juven, T., Barak, Y., Zauberman, A., George, D.L., and Oren, M. (1993). Wild type p53 can mediate sequence-specific transactivation of an internal promoter within the mdm2 gene. Oncogene *8*, 3411–3416.

Kitevska, T., Spencer, D.M.S., and Hawkins, C.J. (2009). Caspase-2: controversial killer or checkpoint controller? Apoptosis *14*, 829–848.

Krumschnabel, G., Manzl, C., and Villunger, A. (2009a). Caspase-2: killer, savior and safeguard—emerging versatile roles for an ill-defined caspase. Oncogene *28*, 3093–3096.

Krumschnabel, G., Sohm, B., Bock, F., Manzl, C., and Villunger, A. (2009b). The enigma of caspase-2: the laymen's view. Cell Death Differ. *16*, 195–207.

Kruse, J.-P., and Gu, W. (2009). Modes of p53 regulation. Cell *137*, 609–622.

Kubbutat, M.H., Jones, S.N., and Vousden, K.H. (1997). Regulation of p53 stability by Mdm2. Nature *387*, 299–303.

Kumar, S. (2009). Caspase 2 in apoptosis, the DNA damage response and tumour suppression: enigma no more? Nat. Rev. Cancer *9*, 897–903.

Lahav, G., Rosenfeld, N., Sigal, A., Geva-Zatorsky, N., Levine, A.J., Elowitz, M.B., and Alon, U. (2004). Dynamics of the p53-Mdm2 feedback loop in individual cells. Nat. Genet. *36*, 147–150.

Lin, Y., Ma, W., and Benchimol, S. (2000). Pidd, a new death-domain-containing protein, is induced by p53 and promotes apoptosis. Nat. Genet. *26*, 122–127.

Loewer, A., Batchelor, E., Gaglia, G., and Lahav, G. (2010). Basal dynamics of p53 reveal transcriptionally attenuated pulses in cycling cells. Cell *142*, 89–100.

Logette, E., Schuepbach-Mallepell, S., Eckert, M.J., Leo, X.H., Jaccard, B., Manzl, C., Tardivel, A., Villunger, A., Quadroni, M., Gaide, O., and Tschopp, J. (2011). PIDD orchestrates translesion DNA synthesis in response to UV irradiation. Cell Death Differ. *18*, 1036–1045.

Lu, X. (2010). Tied up in loops: positive and negative autoregulation of p53. Cold Spring Harb Perspect Biol *2*, a000984.

Mancini, M., Machamer, C.E., Roy, S., Nicholson, D.W., Thornberry, N.A., Casciola-Rosen, L.A., and Rosen, A. (2000). Caspase-2 is localized at the Golgi complex and cleaves golgin-160 during apoptosis. J. Cell Biol. *149*, 603–612.

Manfredi, J.J. (2010). The Mdm2-p53 relationship evolves: Mdm2 swings both ways as an oncogene and a tumor suppressor. Genes Dev. *24*, 1580–1589.

Marine, J.C., and Lozano, G. (2010). Mdm2-mediated ubiquitylation: p53 and beyond. Cell Death Differ. *17*, 93–102.

Menendez, D., Inga, A., and Resnick, M.A. (2009). The expanding universe of p53 targets. Nat. Rev. Cancer *9*, 724–737.

Momand, J., Zambetti, G.P., Olson, D.C., George, D., and Levine, A.J. (1992). The mdm-2 oncogene product forms a complex with the p53 protein and inhibits p53-mediated transactivation. Cell *69*, 1237–1245.

Oliver, T.G., Mercer, K.L., Sayles, L.C., Burke, J.R., Mendus, D., Lovejoy, K.S., Cheng, M.-H., Subramanian, A., Mu, D., Powers, S., et al. (2010). Chronic cisplatin treatment promotes enhanced damage repair and tumor progression in a mouse model of lung cancer. Genes Dev. *24*, 837–852.

Pan, Y., and Chen, J. (2003). MDM2 promotes ubiquitination and degradation of MDMX. Mol. Cell. Biol. *23*, 5113–5121.

Park, H.H., Logette, E., Raunser, S., Cuenin, S., Walz, T., Tschopp, J., and Wu, H. (2007). Death domain assembly mechanism revealed by crystal structure of the oligomeric PIDDosome core complex. Cell *128*, 533–546.

Pochampally, R., Fodera, B., Chen, L., Shao, W., Levine, E.A., and Chen, J. (1998). A 60 kd MDM2 isoform is produced by caspase cleavage in non-apoptotic tumor cells. Oncogene *17*, 2629–2636.

Pochampally, R., Fodera, B., Chen, L., Lu, W., and Chen, J. (1999). Activation of an MDM2-specific caspase by p53 in the absence of apoptosis. J. Biol. Chem. *274*, 15271–15277.

Tanimura, S., Ohtsuka, S., Mitsui, K., Shirouzu, K., Yoshimura, A., and Ohtsubo, M. (1999). MDM2 interacts with MDMX through their RING finger domains. FEBS Lett. *447*, 5–9.

Tinel, A., and Tschopp, J. (2004). The PIDDosome, a protein complex implicated in activation of caspase-2 in response to genotoxic stress. Science *304*, 843–846.

Tinel, A., Janssens, S., Lippens, S., Cuenin, S., Logette, E., Jaccard, B., Quadroni, M., and Tschopp, J. (2007). Autoproteolysis of PIDD marks the bifurcation between pro-death caspase-2 and pro-survival NF-kappaB pathway. EMBO J. *26*, 197–208.

Tu, S., McStay, G.P., Boucher, L.-M., Mak, T., Beere, H.M., and Green, D.R. (2006). In situ trapping of activated initiator caspases reveals a role for caspase-2 in heat shock-induced apoptosis. Nat. Cell Biol. *8*, 72–77.

Upton, J.-P., Austgen, K., Nishino, M., Coakley, K.M., Hagen, A., Han, D., Papa, F.R., and Oakes, S.A. (2008). Caspase-2 cleavage of BID is a critical apoptotic signal downstream of endoplasmic reticulum stress. Mol. Cell. Biol. *28*, 3943–3951.

Vakifahmetoglu-Norberg, H., and Zhivotovsky, B. (2010). The unpredictable caspase-2: what can it do? Trends Cell Biol. *20*, 150–159.

Ventura, A., Kirsch, D.G., McLaughlin, M.E., Tuveson, D.A., Grimm, J., Lintault, L., Newman, J., Reczek, E.E., Weissleder, R., and Jacks, T. (2007). Restoration of p53 function leads to tumour regression in vivo. Nature *445*, 661–665.

Vilborg, A., Glahder, J.A., Wilhelm, M.T., Bersani, C., Corcoran, M., Mahmoudi, S., Rosenstierne, M., Grandér, D., Farnebo, M., Norrild, B., and Wiman, K.G. (2009). The p53 target Wig-1 regulates p53 mRNA stability through an AU-rich element. Proc. Natl. Acad. Sci. USA *106*, 15756–15761.

Vousden, K.H. (2006). Outcomes of p53 activation—spoilt for choice. J. Cell Sci. *119*, 5015–5020.

Wade, M., Wang, Y.V., and Wahl, G.M. (2010). The p53 orchestra: Mdm2 and Mdmx set the tone. Trends Cell Biol. *20*, 299–309.

Wu, X., Bayle, J.H., Olson, D., and Levine, A.J. (1993). The p53-mdm-2 autoregulatory feedback loop. Genes Dev. *7* (7A), 1126–1132.

Yang, H.-Y., Wen, Y.-Y., Chen, C.-H., Lozano, G., and Lee, M.-H. (2003). 14-3-3 sigma positively regulates p53 and suppresses tumor growth. Mol. Cell. Biol. *23*, 7096–7107.

Zhang, Y., Wolf, G.W., Bhat, K., Jin, A., Allio, T., Burkhart, W.A., and Xiong, Y. (2003). Ribosomal protein L11 negatively regulates oncoprotein MDM2 and mediates a p53-dependent ribosomal-stress checkpoint pathway. Mol. Cell. Biol. *23*, 8902–8912.